

Configuration-interaction approach to hole pairing in the two-dimensional Hubbard model

E. Louis

Departamento de Física Aplicada, Universidad de Alicante, Apartado 99, E-03080 Alicante, Spain

F. Guinea, M. P. López Sancho, and J. A. Vergés

Instituto de Ciencia de Materiales de Madrid, CSIC, Cantoblanco, E-28049 Madrid, Spain

(Received 17 November 1998)

The interactions between holes in the Hubbard model, in the low density, intermediate- to strong-coupling limit, are investigated by systematically improving mean field calculations. The configuration-interaction basis set is constructed by applying to local unrestricted Hartree-Fock configurations all lattice translations and rotations. It is shown that this technique reproduces, correctly, the properties of the Heisenberg model, in the limit of large U . Upon doping, dressed spin polarons in neighboring sites have an increased kinetic energy and an enhanced hopping rate. Both effects are of the order of the hopping integral and lead to an effective attraction at intermediate couplings. The numerical results also show that when more than two holes are added to the system, they do not tend to cluster, but rather hole pairs remain far apart. Hole-hole correlations are also calculated and shown to be in qualitative agreement with exact calculations for 4×4 clusters. In particular our results indicate that for intermediate coupling the hole-hole correlation attains a maximum when the holes are in the same sublattice at a distance of $\sqrt{2}$ times the lattice spacing, in agreement with exact results and the t - J model. The method is also used to derive known properties of the quasiparticle band structure of isolated spin polarons. [S0163-1829(99)15221-4]

I. INTRODUCTION

The nature of the low-energy excitations in the Hubbard model has attracted a great deal of attention. It is well established that at half-filling the ground state is an antiferromagnetic (AF) insulator. Also, there exists conclusive evidence which indicates that antiferromagnetism is rapidly suppressed upon doping.^{1,2} Close to half-filling, a large amount of work suggests the existence of spin polarons, made of dressed holes, which propagate within a given sublattice with kinetic energy which in the strong-coupling limit is of the order of $J = 4t^2/U$,^{3,4} where t is the hopping integral and U the on-site Coulomb repulsion. These results are consistent with similar calculations in the strong-coupling, low-doping limit of the Hubbard model, the t - J model.⁵⁻⁷ There is also evidence for an effective attraction between these spin polarons.⁸⁻¹⁴ However, recent and extensive Monte Carlo calculations for 0.85 filling and $U = 2t - 8t$ have shown that the pairing correlations vanish as the system size or the interaction strength increases.¹⁵

We have recently analyzed the dynamics of spin polarons^{16,17} and the interactions between them¹⁸ by means of a systematic expansion around mean field calculations of the Hubbard model. Two spin polarons in neighboring sites experience an increase in their internal kinetic energy, due to the overlap of the charge cloud. This repulsion is of the order of t . In addition, a polaron reduces the obstacles for the diffusion of another, leading to an assisted hopping term which is also of the same order. The combination of these effects is an attractive interaction at intermediate values of U/t . The purpose of this work is to discuss in detail the results and the approach proposed in Ref. 18. We present new results which support the validity of our approach, highlighting the physically appealing picture of pairing that it provides. An alter-

native scheme to go beyond the unrestricted Hartree-Fock (UHF) approximation is to supplement it with the Gutzwiller projection method or, equivalently, slave boson techniques.^{19,20} These results are in agreement with the existence of significant effects due to the delocalization of the solutions, as reported here.

The rest of the paper is organized as follows. In Sec. II we discuss the physical basis of our proposal and the way in which we implement the configuration-interaction method. A discussion of the limit of large U/t in the undoped case is presented in Sec. III. It is shown that, contrary to some expectations, the Hartree-Fock scheme reproduces correctly the mean field solution of the Heisenberg model. The systematic corrections analyzed here can be put in precise correspondence with similar terms discussed for quantum antiferromagnets. Results for the 4×4 cluster are compared with exact results in Sec. IV. Section V is devoted to a discussion of our results for a single hole (spin polaron) and for two or more holes. The hole-hole correlations are also presented in this section. The last section is devoted to the conclusions of our work.

II. METHODS

A. Hamiltonian

We investigate the simplest version of the Hubbard Hamiltonian used to describe the dynamics of electrons in CuO_2 layers, namely,

$$H = T + C, \quad (1a)$$

$$T = \sum_{\sigma} T^{\sigma} = - \sum_{\sigma, \langle ij \rangle} t_{ij} c_{i\sigma}^{\dagger} c_{j\sigma}, \quad (1b)$$

$$C = \sum_i U_i n_{i\uparrow} n_{i\downarrow}. \quad (1c)$$

The Hamiltonian includes a single atomic orbital per lattice site with energy $E_i=0$. The sums are over all lattice sites $i = 1, \dots, N_s$ of the chosen cluster of the square lattice and/or the z component of the spin ($\sigma = \uparrow, \downarrow$). The operator $c_{j\sigma}$ destroys an electron of spin σ at site j , and $n_{i\sigma} = c_{i\sigma}^\dagger c_{i\sigma}$ is the local density operator. t_{ij} is the hopping matrix element between sites i and j (the symbol $\langle ij \rangle$ denotes that the sum is restricted to all nearest neighbor pairs) and U_i is the intrasite Coulomb repulsion. Here we take $t_{ij} = t$ and $U_i = U$, and the lattice constant as the unit of length.

B. Unrestricted Hartree-Fock solutions

As we shall only consider UHF solutions having a local magnetization pointing in the same direction everywhere in the cluster, we shall use the most simple version of the UHF approximation.²¹ Within this approximation the effective mean field Hamiltonian that accounts for the Hubbard term is written as

$$C^{\text{eff}} = \sum_{\sigma} X^{\sigma} - U \sum_i \langle n_{i\uparrow} \rangle \langle n_{i\downarrow} \rangle, \quad (2a)$$

$$X^{\sigma} = U \sum_i n_{i\sigma} \langle n_{i\bar{\sigma}} \rangle. \quad (2b)$$

The full UHF Hamiltonian is then written as

$$H^{\text{UHF}} = T + C^{\text{eff}}. \quad (3)$$

Use of the UHF approximation in finite clusters provides a first-order approximation to the spin polaron near half-filling. As discussed elsewhere, the UHF approximation describes well the undoped, insulating state at half-filling²¹ (see also the next section). A realistic picture of the spin-wave excitations is obtained by adding harmonic fluctuations by means of the time-dependent Hartree-Fock approximation [random phase approximation (RPA)].²² At intermediate and large values of U/t , the most stable HF solution with a single hole is a spin polaron.^{21,16} In this solution, approximately half of the charge of the hole is located at a given site. The spin at that site is small and it is reversed with respect to the antiferromagnetic background. The remaining charge is concentrated in the four neighboring sites. A number of alternative derivations lead to a similar picture of this small spin bag.^{23–26} A similar solution is expected to exist in the t - J model.

A schematic picture of the initial one- and two-hole Hartree-Fock wave functions used in this work is shown in Fig. 1. They represent the solutions observed at large values of U/t for the isolated polaron and two spin polarons on neighboring sites. The electronic spectrum of these configurations shows localized states which split from the top of the valence band.

As usual in mean field theories, the UHF solution for an arbitrary number of holes,²¹ such as the spin polaron solution described above, breaks symmetries which must be restored by quantum fluctuations. In particular, it breaks spin symmetry and translational invariance (see Fig. 1). Spin isotropy

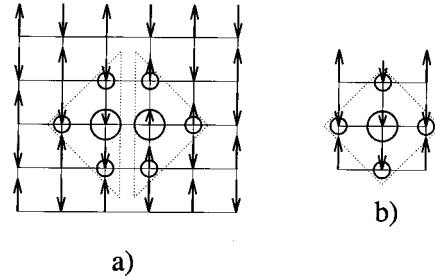


FIG. 1. (a) Sketch of one of the bipolaron solutions, at large values of U/t , considered in the text. Circles denote the local charge, measured from half-filling, and arrows denote the spins. There are two localized states marked by the dashed line. For comparison, the single-polaron solution is shown in (b).

must exist in finite clusters. However, it is spontaneously broken in the thermodynamic limit, due to the presence of the antiferromagnetic background. Hence, we do not expect that the lack of spin invariance is a serious drawback of the Hartree-Fock solutions (this point is analyzed in some detail in Ref. 22). Results obtained for small clusters^{17,27} show a slight improvement of the energy, which goes to zero as the cluster size is increased. On the other hand, translational invariance is expected to be present in the exact solution of clusters of any size. The way we restore translational invariance is discussed in the following subsection. Finally we show how to estimate the effects due to zero-point fluctuations around the UHF ground state.²² For spin polarons these corrections do not appreciably change the results, although they are necessary to describe the long-range magnon cloud around the spin polaron.²⁸

C. Configuration-interaction method

We have improved the mean field results by following a procedure suggested years ago by some of us.¹⁶ We hybridize a given spin UHF solution with all wave functions obtained from it by lattice translations. In the case of two or more holes point symmetry has also to be restored. This is accomplished by applying rotations to the chosen configuration. Configurations generated from a given one through this procedure are degenerate in energy and interact strongly. Here we have also investigated the effect of extending the basis by including other configurations having different energies. In all cases we include sets of wave functions with the lattice symmetry restored as mentioned.

In a path integral formulation, this procedure would be similar to calculating the contribution from instantons which visit different minima. On the other hand, it is equivalent to the configuration interaction (CI) method used in quantum chemistry. The CI wave function for a solution corresponding to N_e electrons is then written as

$$\Psi(N_e) = \sum_i a_i \Phi^i(N_e), \quad (4)$$

where the set $\Phi^i(N_e)$ is formed by some chosen UHF wave functions (Slater determinants) plus those obtained from them by all lattice translations and rotations. The coefficients a_i are obtained through diagonalization of the exact Hamiltonian. The same method, using homogeneous paramagnetic

solutions as starting point, has been used in Ref. 29. The wave functions forming this basis set are not in principle orthogonal. Thus, the wave function overlap has to be taken into account in the calculation of the matrix elements of the Hamiltonian.

If only configurations having the same energy and corresponding, thus, to the same UHF Hamiltonian are included, a physically sound decomposition of the exact Hamiltonian is the following:¹⁷

$$H = H^{\text{UHF}} + C - \sum_{\sigma} X^{\sigma} + U \sum_i \langle n_{i\uparrow} \rangle \langle n_{i\downarrow} \rangle. \quad (5)$$

In writing the matrix elements of this Hamiltonian we should note that the basis formed by the wave functions Φ_i is not orthogonal. Then, we obtain

$$H_{ij} = \left(E^{\text{UHF}} + U \sum_i \langle n_{i\uparrow} \rangle \langle n_{i\downarrow} \rangle \right) S_{ij} + C_{ij} - \sum_{\sigma} X_{ij}^{\sigma} S_{ij}^{\bar{\sigma}}, \quad (6)$$

where E^{UHF} is the UHF energy of a given mean field solution, and the matrix elements of the overlap S are given by

$$S_{ij} = \langle \Phi^i(N_e) | \Phi^j(N_e) \rangle = S_{ij}^{\uparrow} S_{ij}^{\downarrow}. \quad (7)$$

This factorization is a consequence of the characteristics of the mean field solutions considered in this work (only one component of the spin different from zero). The specific expression for the matrix elements of the overlap is

$$S_{ij}^{\sigma} = \begin{vmatrix} \langle \phi_1^{i\sigma} | \phi_1^{j\sigma} \rangle & \cdots & \langle \phi_1^{i\sigma} | \phi_{N_{\sigma}}^{j\sigma} \rangle \\ \cdots & \cdots & \cdots \\ \langle \phi_{N_{\sigma}}^{i\sigma} | \phi_1^{j\sigma} \rangle & \cdots & \langle \phi_{N_{\sigma}}^{i\sigma} | \phi_{N_{\sigma}}^{j\sigma} \rangle \end{vmatrix}, \quad (8)$$

where the number of particles for each component of the spin is determined from the usual conditions $N_{\uparrow} + N_{\downarrow} = N_e$ and $N_{\uparrow} - N_{\downarrow} = 2S_z$. The $\phi_n^{i\sigma}$ are the mono-electronic wave functions corresponding to the Slater determinant i ,

$$|\phi_n^{i\sigma}\rangle = \sum_k \alpha_{nk}^{i\sigma} c_{k\sigma}^{\dagger} |0\rangle, \quad (9)$$

$\alpha_{nk}^{i\sigma}$ being real coefficients obtained through diagonalization of the H^{UHF} Hamiltonian. The matrix element of the exchange operator between Slater determinants i and j is

$$X_{ij}^{\sigma} = \begin{vmatrix} \langle \phi_1^{i\sigma} | X^{\sigma} \phi_1^{j\sigma} \rangle & \cdots & \langle \phi_1^{i\sigma} | \phi_{N_{\sigma}}^{j\sigma} \rangle \\ \cdots & \cdots & \cdots \\ \langle \phi_{N_{\sigma}}^{i\sigma} | X^{\sigma} \phi_1^{j\sigma} \rangle & \cdots & \langle \phi_{N_{\sigma}}^{i\sigma} | \phi_{N_{\sigma}}^{j\sigma} \rangle \end{vmatrix} \\ + \cdots + \begin{vmatrix} \langle \phi_1^{i\sigma} | \phi_1^{j\sigma} \rangle & \cdots & \langle \phi_1^{i\sigma} | X^{\sigma} \phi_{N_{\sigma}}^{j\sigma} \rangle \\ \cdots & \cdots & \cdots \\ \langle \phi_{N_{\sigma}}^{i\sigma} | \phi_1^{j\sigma} \rangle & \cdots & \langle \phi_{N_{\sigma}}^{i\sigma} | X^{\sigma} \phi_{N_{\sigma}}^{j\sigma} \rangle \end{vmatrix}, \quad (10)$$

where the matrix elements of X^{σ} between mono-electronic wave functions are given by

$$\langle \phi_n^{i\sigma} | X^{\sigma} \phi_m^{j\sigma} \rangle = U \sum_k \alpha_{nk}^{i\sigma} \alpha_{mk}^{j\sigma} \langle n_{k\bar{\sigma}} \rangle. \quad (11)$$

On the other hand, the matrix elements of C are

$$C_{ij} = U \sum_k (n_{k\uparrow})_{ij} (n_{k\downarrow})_{ij}, \quad (12)$$

where each $(n_{k\sigma})_{ij}$ is given by an equation similar to Eq. (10). The matrix elements of the density operator between mono-electronic wave functions are

$$\langle \phi_n^{i\sigma} | n_{k\sigma} \phi_m^{j\sigma} \rangle = \alpha_{nk}^{i\sigma} \alpha_{mk}^{j\sigma}. \quad (13)$$

If the CI basis includes wave functions having different UHF energies, the above procedure is not valid and one should calculate the matrix elements of the original exact Hamiltonian. Although this is in fact reduced to calculating the matrix elements of the kinetic energy operator T , the procedure is slightly more costly (in terms of computer time) than the one described above. The matrix elements of the exact Hamiltonian in the basis of Slater determinants are

$$H_{ij} = \sum_{\sigma} T_{ij}^{\sigma} S_{ij}^{\bar{\sigma}} + C_{ij}, \quad (14)$$

where T_{ij}^{σ} are given by an equation similar to Eq. (10), and the matrix elements of the kinetic energy operator between mono-electronic wave functions are

$$\langle \phi_n^{i\sigma} | T^{\sigma} \phi_m^{j\sigma} \rangle = -t \sum_{\langle kl \rangle} \alpha_{nk}^{i\sigma} \alpha_{ml}^{j\sigma}. \quad (15)$$

The matrix elements involved in the calculation of hole-hole correlations for a given CI wave function are similar to those that appeared in the computation of the Hubbard term. In particular the following expectation value has to be computed:

$$\langle \Psi | (1 - n_k)(1 - n_l) | \Psi \rangle = \sum_{ij} a_i a_j \langle \Phi_i | (1 - n_k)(1 - n_l) | \Phi_j \rangle, \quad (16)$$

where $n_k = n_{k\uparrow} + n_{k\downarrow}$. The terms of the four operators in this expectation value are similar to Eq. (12). Those requiring more computer time involve $n_{k\uparrow} n_{l\uparrow}$ with $k \neq l$,

$$(n_{k\uparrow} n_{l\uparrow})_{ij} \\ = \begin{vmatrix} \langle \phi_1^{i\sigma} | n_{k\uparrow} \phi_1^{j\sigma} \rangle & \langle \phi_1^{i\sigma} | n_{l\uparrow} \phi_2^{j\sigma} \rangle & \cdots & \langle \phi_1^{i\sigma} | \phi_{N_{\sigma}}^{j\sigma} \rangle \\ \cdots & \cdots & \cdots & \cdots \\ \langle \phi_{N_{\sigma}}^{i\sigma} | n_{k\uparrow} \phi_1^{j\sigma} \rangle & \langle \phi_{N_{\sigma}}^{i\sigma} | n_{l\uparrow} \phi_2^{j\sigma} \rangle & \cdots & \langle \phi_{N_{\sigma}}^{i\sigma} | \phi_{N_{\sigma}}^{j\sigma} \rangle \end{vmatrix} \\ + \text{permutations}. \quad (17)$$

D. Numerical calculations

Calculations have been carried out on $L \times L$ clusters with periodic boundary conditions ($L \leq 12$) and $U = 8t - 5000t$. Some results for lower values of U are also presented. Note that $U = 8t$ is widely accepted as the most physically meaningful value of Coulomb repulsion in these systems (see, for instance, Ref. 30). Although larger clusters can be easily

TABLE I. Exact (Ref. 8), UHF, and CI (see text) energies of the Hubbard model vs U , for the half-filled 4×4 cluster. All energies are given in units of the hopping integral t . The UHF solution of lowest energy corresponds to the antiferromagnetic configuration while the CI results were obtained by adding to the AF configuration the 32 configurations having two neighboring spins flipped (referred to as sf). The interaction and overlap between the AF and the sf configurations ($S_{\text{AF,sf}}$ and $t_{\text{AF,sf}}$) are also given.

U/t	Exact	UHF		CI		
	Exact	AF	sf	AF+sf	$t_{\text{AF,sf}}$	$S_{\text{AF,sf}}$
6	-10.55222	-9.37989	-7.94663	-9.85296	1.1410	0.1035
8	-8.46887	-7.38963	-6.16154	-7.87777	0.5863	0.0572
16	-4.61186	-3.91165	-3.20231	-4.27171	0.1692	0.0150
32	-2.37589	-1.98846	-1.61884	-2.19194	0.0682	0.0039
50	-1.53078	-1.27695	-1.03838	-1.41060	0.0415	0.0016
100	-	-0.63962	-0.51980	-0.70736	0.0202	0.0004

reached, no improvement of the results is achieved due to the short-range character of the interactions (see below).

The numerical procedure runs as follows. Localized UHF solutions are first obtained and the Slater determinants for a given filling constructed. The full CI basis set is obtained by applying all lattice translations to the chosen localized UHF Slater determinants all having the same z component of the spin S_z . Then we calculate the matrix elements of the overlap and of the Hamiltonian in that basis set. This is by far the most time-consuming part of the whole calculation. Diagonalization is carried out by means of standard subroutines for nonorthogonal bases. The state of lowest energy corresponds to the CI ground state of the system for a given S_z . The desired expectation values are calculated by means of this ground state wave function. The procedure is variational and, thus, successive enlargements of the basis set always improve the description of the ground state.

III. LIMIT OF LARGE U IN THE UNDOPED CASE

The Hartree-Fock scheme, for the undoped Hubbard model in a square lattice, gives an antiferromagnetic ground state, with a charge gap. At large values of U/t , the gap is of order U . The simplest correction beyond Hartree-Fock, the RPA approximation, leads to a continuum of spin waves at low energies.²² Thus, the qualitative features of the solution are in good agreement with the expected properties of an antiferromagnetic insulator.

There is, however, a great deal of controversy regarding the adequacy of mean field techniques in describing a Mott insulator.^{31,32} In principle, the Hubbard model, in the large- U limit, should describe well such a system. At half-filling and large U , the only low-energy degrees of freedom of the Hubbard model are the localized spins, which interact antiferromagnetically, with coupling $J=4t^2/U$. It has been argued that, as long-range magnetic order is not relevant for the existence of the Mott insulator, spin systems with a spin gap are the most generic realization of this phase. A spin gap is often associated with the formation of a resonating valence bond (RVB)-like state, which cannot be adiabatically connected to the Hartree-Fock solution of the Hubbard model. So far, the best examples showing these features are two-leg spin-1/2 ladders.³⁴ Recent work³³ indicates that, in the presence of magnetic order, the metal-insulator transition is of

the Slater type; that is, coherent quasiparticles can always be defined in the metallic side. These results seem to favor the scenario suggested in Ref. 31, and lend support to our mean-field-plus corrections approach.

Without entering into the full polemic outlined above, we now show that the method used here gives, in full detail, the results which can be obtained from the Heisenberg model by expanding around the antiferromagnetic mean field solution.³⁵ Such an expansion gives a consistent picture of the physics of the Heisenberg model in a square lattice.

The ground state energy of the Hartree-Fock solution in a 4×4 cluster is compared to the exact value⁸ at large values of U in Table I. The corresponding Heisenberg model is

$$H_{\text{Heis}} = \frac{4t^2}{U} \sum_{ij} \tilde{\mathbf{S}}_i \cdot \tilde{\mathbf{S}}_j - \frac{t^2}{U} \sum_{ij} n_i n_j. \quad (18)$$

In a 4×4 cluster, the exact ground state energy is

$$E_{\text{Heis}} = -16(c+0.5) \frac{4t^2}{U}, \quad (19)$$

where $c=0.702$,³⁶ in good agreement with the results for the Hubbard model. The mean field energy can be parametrized in the same way, except that $c=0.5$. This is the result that one expects for the mean field solution of the Heisenberg model, which is given by a staggered configuration of static spins. This solution can be viewed as the ground state of an anisotropic Heisenberg model with $J_z=J$ and $J_{\pm}=0$.

We now analyze corrections to the Hartree-Fock solution by hybridizing it with mean field wave functions obtained from it by flipping two neighboring spins (hereafter referred to as “sf”). These solutions are local extrema of the mean field solutions in the large- U limit. In Table I we show the energy difference between these states and the AF Hartree-Fock ground state, and their overlap and matrix element also with the ground state. We have checked that these are the only wave functions with a non-negligible mixing with the ground state. The overlap goes rapidly to zero, and the energy difference and matrix elements adjust well to the expressions

$$\Delta E_{\text{AF,sf}} = E_{\text{AF}} - E_{\text{sf}} = \frac{12t^2}{U}, \quad (20a)$$

TABLE II. UHF and CI (see text) energies of the Hubbard model in the 4×4 cluster for several values of U and one and two holes (with respect to half-filling). All energies are given in units of the hopping integral t . The CI results for two holes were obtained by including all configurations having the holes separated by vectors of the set $\{1,0\}$ or $\{2,1\}$. The CI calculation for one hole includes the spin polaron configuration. In both cases the full basis set was constructed by restoring point and translational symmetries.

U	One hole		Two holes			
	UHF	CI	UHF-(1,0)	CI-{1,0}	UHF-(2,1)	CI-{2,1}
4	-13.30222	-13.36021	-14.09307	-14.20511	-14.09240	-14.16640
6	-10.27549	-10.59418	-11.18149	-11.65669	-11.12471	-11.55214
8	-8.46151	-8.76271	-9.47288	-9.94496	-9.47043	-9.81703
16	-5.37431	-5.53656	-6.59120	-7.08701	-6.79804	-6.97274
32	-3.70563	-3.78024	-5.04100	-5.54390	-5.40559	-5.48360
50	-3.09365	-3.13879	-4.47406	-4.97558	-4.90015	-4.94714

$$t_{\text{AF,sf}} = \frac{2t^2}{U}. \quad (20b)$$

These are the results that one obtains when proceeding from the Heisenberg model. These values, inserted in a perturbative analysis of quantum corrections to the ground state energy of the Heisenberg model,³⁵ lead to excellent agreement with exact results (see also below).

As already pointed out, in the CI calculation of the ground state energy we only include the mean field wave functions with two neighboring spins flipped. Restoring point symmetry gives a total of 4 configurations, while applying lattice translations leads to a set of $4L^2/2$ configurations (remember that configurations on different sublattices do not interact) to which the AF wave function has to be added. In the case of the 4×4 cluster the set has a total of 33 configurations. The CI energy for this cluster is given in Table I along with the exact and the UHF energies. It is noted that the CI calculation reduces in 50% the difference between the exact and the mean field result. Improving this result would require including a very large set, as other configurations only decrease the ground state energy very slightly.

In the large- U limit, the largest interaction is $t_{\text{AF,sf}}$. Then, neglecting the overlap between the AF and the sf mean field solutions, the CI energy of the ground state can be approximated by

$$E_{\text{CI}} = \frac{1}{2} \left[E_{\text{AF}} + E_{\text{sf}} - \Delta E_{\text{AF,sf}} \sqrt{1 + \frac{8L^2 t_{\text{AF,sf}}^2}{(\Delta E_{\text{AF,sf}})^2}} \right]. \quad (21)$$

For $U = 50t$ this expression gives $E_{\text{CI}} = -1.421$, in excellent agreement with the CI result given in Table I.

Note that a perturbative calculation of the corrections of the ground state energy in finite clusters is somewhat tricky, as the matrix element scales with $\sqrt{N_s}$, where $N_s = L^2$ is the number of sites in the cluster, while the energy difference is independent of N_s . The first term in a perturbative expansion (pe) coincides with the first term in the expansion of the square root in Eq. (21),

$$E_{\text{pe}} = E_{\text{AF}} - \frac{2L^2 t_{\text{AF,sf}}^2}{\Delta E_{\text{AF,sf}}}, \quad (22)$$

in agreement with the result reported in Ref. 35. Although this correction to the AF energy has the expected size dependence for an extensive magnitude (it is proportional to the number of sites N_s) and gives an energy already very similar to the exact, it was obtained by inconsistently expanding in terms of a parameter that can be quite large. For instance, in the 4×4 cluster and $U = 50t$, $E_{\text{pe}} \approx 1.51$, close to the exact result (Table I), while $(8L^2 t_{\text{AF,sf}}^2)/(\Delta E_{\text{AF,sf}})^2 \approx 3.9$, much larger than 1. Thus, perturbation theory is doomed to fail even for rather small clusters.

On the other hand, the CI calculation described above introduces a correction to the AF energy which does not have the correct size dependence. This can be easily checked in the large-cluster limit in which the CI energy can be approximated by

$$E_{\text{CI}} \approx \frac{1}{2} (E_{\text{AF}} + E_{\text{sf}}) - \sqrt{2} L t_{\text{AF,sf}}, \quad (23)$$

while the correct expression should scale as N_s , because, in large clusters, the difference between the exact and the Hartree-Fock ground state energies must be proportional to N_s , irrespective of the adequacy of the Hartree-Fock approximation.

Thus, one obtains a better approximation to the ground state energy in the thermodynamic limit, by using the perturbative calculations in small clusters and extrapolating them to large clusters, as in the related t - J model.³⁵ In any case, the problem outlined here does not appear when calculating corrections to localized spin textures, such as the one- and two-spin polarons analyzed in the next sections. The relevant properties are associated with the size of the texture, and do not scale with the size of the cluster they are embedded in.

From the previous analysis, we can safely conclude that our scheme gives a reliable approximation to the undoped Hubbard model in a square lattice in the strong-coupling regime $U/t \gg 1$. We cannot conclude whether the method is adequate or not for the study of models which exhibit a spin gap. It should be noted, however, that a spin gap need not only be related to RVB states like ground states. A spin system modeled by the nonlinear σ model can also exhibit a gap in the ground state, if quantum fluctuations, due to dimensionality or frustration, are sufficiently large. In this

TABLE III. Exact (Ref. 8) and UHF or CI (see text) energies of the Hubbard model in 4×4 clusters for several values of U one or two holes (with respect to half-filling). All energies are given in units of the hopping integral t . The CI results for two holes were obtained by including all $\{1,0\}$ and $\{2,1\}$ configurations (see also caption of Table II).

U/t	Exact		CI	
	One hole	Two holes	One hole	Two holes
4	-14.66524	-15.74459	-13.36021	-14.48135
6	-11.96700	-13.42123	-10.59418	-11.81262
8	-10.14724	-11.86883	-8.76271	-10.17505
16	-6.80729	-9.06557	-5.53656	-7.21100
32	-4.93556	-7.56832	-3.78024	-5.59560
50	-4.25663	-7.07718	-3.13879	-5.00862

case, a mean field approach plus leading quantum corrections should be qualitatively correct.

IV. COMPARISON WITH EXACT RESULTS FOR 4×4 CLUSTERS WITH TWO HOLES

In order to evaluate the performance of our approach we have calculated the ground state energy of two holes in the 4×4 cluster and compared the results with those obtained by means of the Lanczos method.⁸ The results are reported in Tables II–IV, where the energies for one hole are also given for the sake of completeness (a full discussion of this case can be found in Ref. 16; see also below). In the case of one hole the standard spin polaron solution (Fig. 1) and those derived from it through lattice translations form the basis set. For two holes we consider solutions with $S_z = 0$ or 1. In the first case we include either the configuration having the two holes at the shortest distance, i.e., separated by a $(1,0)$ vector³⁷ and/or at the largest distance possible, that is, separated by a $(2,1)$ vector, and those obtained from them through rotations. The basis used for the two polarons at the shortest distance is shown in Fig. 2. The set of these four configurations has the proper point symmetry. Again, lattice translations are applied to these configurations to produce a basis set with full translational symmetry. On the other hand, wave functions with $S_z = 1$ can be constructed by including configurations with the two holes separated by vectors $(1,1)$ and/or $(2,2)$.

TABLE IV. Same as Table II for two holes wave functions with $S_z = 1$. The energy of the CI solution corresponding to $(2,2)$ almost coincides with that of its UHF solution. Including all configurations of the sets $\{1,1\}$ and $\{2,2\}$ does not change the result obtained with only the former set.

U/t	UHF		CI
	$(1,1)$	$(2,2)$	$\{1,1\}$
6	-11.12980	-10.89495	-11.77834
8	-9.48701	-9.37275	-10.11391
16	-6.77454	-6.78954	-7.10740
32	-5.33285	-5.41009	-5.48456
50	-4.80587	-4.90506	-4.89772

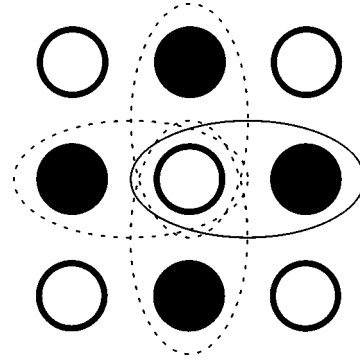


FIG. 2. Sketch of the bipolaron UHF wave functions used in this work. Note that the four wave functions are obtained by successive rotations of $\pi/2$. The complete basis set is produced by translation of these wave functions through the whole cluster.

The results for the energies of wave functions with $S_z = 0$ for several values of the interaction parameter U are reported in Tables II and III. As found for a single hole, the kinetic energy, included by restoring the lattice symmetry, improves the wave function energies.¹⁶ The improvement in the energy is larger for intermediate U . For instance, for $U = 32$ a 10% gain is noted. Within the UHF approximation, the solution with the holes at the largest distance is more favorable for $U > 8t$. Instead, restoring the translational and point symmetries favors a solution with the holes at neighboring sites for all U shown in the tables. The results also indicate that the correction introduced by this procedure does not vanish with U . A more detailed discussion of the physical basis of this result along with results for larger values of U and larger clusters will be presented in the following section. On the other hand, the energies get closer to the exact energies (see Table II). A further improvement in the energy is obtained by including both UHF configurations, namely, $\{1,0\}$ and $\{2,1\}$. This improvement is larger for intermediate U and vanishes as U increases (Table III). Other configurations, such as that proposed in Ref. 47 in which the two holes lie on neighboring sites along a diagonal and a neighboring spin is flipped, may contribute to further improve the CI energy of the ground state.

It is interesting to compare these results with those corresponding to wave functions with $S_z = 1$ also reported in Table IV. It is noted that for $U = 6t - 16t$ the energy of the solution including all configurations from the set $\{1,1\}$ is smaller than those obtained with all configurations from either the set $\{1,0\}$ or the set $\{2,1\}$. However, the wave function constructed with all configurations from the last two sets is more favorable than the best wave function with $S_z = 1$. The latter is in agreement with exact calculations⁸ which obtained a ground state wave function with $S_z = 0$.

V. RESULTS

A. Single polaron

Here we only consider the quasiparticle band structure associated with the single polaron; the energy gain induced through restoration of translational symmetry has been considered elsewhere.¹⁶ The calculated dispersion band of a single polaron is shown in Fig. 3. Because of the antiferromagnetic background, the band has twice the lattice period-

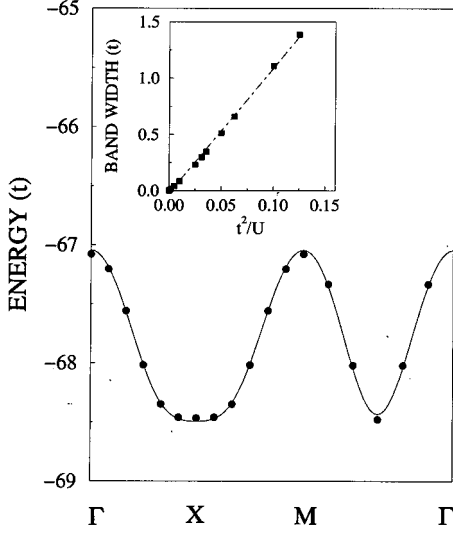


FIG. 3. Quasiparticle band structure for a single hole on 12×12 clusters of the square lattice with periodic boundary conditions and $U=8t$. The solid line corresponds to the fitted dispersion relation (see text). The inset shows the bandwidth as a function of t^2/U for $U \geq 8t$; the fitted straight line is $-0.022t + 11.11t^2/U$.

icity. Exact calculations in finite clusters do not show this periodicity, as the solutions have a well-defined spin and mix different background textures. As cluster sizes are increased, however, exact solutions tend to show the extra periodicity of our results. We interpret this as a manifestation that spin invariance is broken in the thermodynamic limit, because of the antiferromagnetic background. Hence, the lack of this symmetry in our calculations should not induce spurious effects. Figure 3 shows the polaron bandwidth as a function of U . It behaves as t^2/U , the fitted law being

$$E_{\text{BW}} = -0.022t + 11.11 \frac{t^2}{U}. \quad (24)$$

This result indicates that the bandwidth tends to zero as U approaches infinity, as observed in the results for the energy gain reported in Ref. 16. Our scheme allows a straightforward explanation of this scaling. Without reversing the spin of the whole background, the polaron can only hop within a given sublattice. This implies an intermediate virtual hop into a site with an almost fully localized electron of the opposite spin. The amplitude of finding a reversed spin in this new site decays as t^2/U at large U .

On the other hand, we find that the dispersion relation can be satisfactorily fitted by the expression

$$\begin{aligned} \epsilon_{\mathbf{k}} = & \epsilon_0 + 4t_{11}\cos(k_x)\cos(k_y) + 2t_{20}[\cos(2k_x) + \cos(2k_y)] \\ & + 4t_{22}\cos(2k_x)\cos(2k_y) + 4t_{31}[\cos(3k_x)\cos(k_y) \\ & + \cos(k_x)\cos(3k_y)]. \end{aligned} \quad (25)$$

For $U=8t$, we get $t_{11}=0.1899t$, $t_{20}=0.0873t$, $t_{22}=-0.0136t$, and $t_{31}=-0.0087t$. All hopping integrals vanish as t^2/U in the large- U limit for the reason given above. Also the energy gain with respect to the UHF

approximation¹⁷ behaves in this way. All these features are in good agreement with known results^{3-6,14} for both the Hubbard and the t - J models.

The single-hole dispersion in the t - J model is well described by the self-consistent Born approximation,³⁸ which allows for some insight into the physics governing the diffusion of the hole. It has been shown that higher-order corrections are small.³⁹ Within this approximation, nearest neighbor hopping is necessarily accompanied by the absorption, or emission, of a hole. Thus, coherent propagation is only possible after an even number of virtual hoppings, so that the magnons are emitted and absorbed. As in our study, this approximation concludes that the most important effective hoppings are to the $(\pm 1, \pm 1)$ and $(\pm 2, 0)$ neighboring sites (and those equivalent by symmetry). This explains the similarities in the shape of the band in the two approaches. We have also shown that the bandwidth goes, approximately, as $11t^2/U \sim 3J$. Results for the t - J model, for large values of t/J , suggest that the bandwidth goes as $2J$.³⁹⁻⁴¹ This scaling follows from the fact that coherent hopping involves, at least, one spin flip. When $J \leq t$, the spin flip is the slowest process and governs the hopping. The spin flip involves virtual transitions to doubly occupied sites, similar to those considered in our approach. Our results give a somewhat wider band. This is partly due to the fact that, when reducing the Hubbard model to the t - J model for large values of U/t , effective hopping terms are generated, which involve intermediate transitions to doubly occupied sites. These terms are discarded when defining the t - J model. Because of this, the hole propagation must always be reduced in the t - J model with respect to the Hubbard model.

Note, finally, that our results are also similar to those obtained by the self-consistent Born approximation to homogeneous solutions of the Hubbard model itself,⁴² as well as with strong-coupling expansions, similar to the self-consistent Born approximation for the t - J model.⁴³

B. Two holes

We now consider solutions with two spin polarons. The relevant UHF solutions are those with $S_z=0$ (solutions with $S_z=1$ will also be briefly considered). In order for the coupling to be finite, the centers of the two spin polarons must be located in different sublattices. The mean field energy increases as the two polarons are brought closer, although, for intermediate and large values of U , a locally stable Hartree-Fock solution can be found with two polarons at arbitrary distances. We have not attempted to do a full CI analysis of all possible combinations of two holes in a finite cluster. Instead, we have chosen a given mean field solution (UHF) and hybridized it with all others obtained by all lattice translations and rotations. Some results of calculations in which more than one UHF solution are included will be also presented. Clusters of sizes up to 10×10 were studied which, as in the case of the polaron, are large enough due to the short-range interactions between different configurations. The basis used for the two polarons at the shortest distance is shown in Fig. 2. This procedure leads to a set of bands, whose number depends on the number of configurations included in the CI calculation. For instance, if the basis set of Fig. 2 is used, four bands are obtained (see also below).

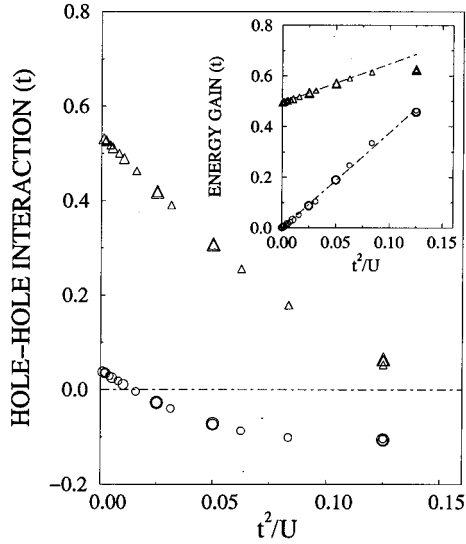


FIG. 4. Comparison of the hole-hole interaction (see main text for the definition) obtained within UHF (triangles) and CI (circles) approximations for wave functions with $S_z=0$. Results correspond to 6×6 , 8×8 , and 10×10 clusters with periodic boundary conditions, and $U \geq 8t$. The size of the symbols increases with increasing cluster size. The inset shows the energy gain due to the inclusion of correlation effects via the CI for both the configuration of holes located in neighboring positions (circles) and holes that are maximally separated in the finite-size cluster (triangles). The respective asymptotic behaviors for large U are $0.495t + 1.53t^2/U$ for holes at the shortest distance and $-0.002t + 3.78t^2/U$ for holes at the largest distance.

As in the single-polaron case, we obtain a gain in energy (with respect to the UHF approximation), due to delocalization of the pair. The numerical results for $L=6, 8$, and 10 and U in the range $8t-5000t$ are shown in the inset of Fig. 4. They can be fitted by the following straight lines:

$$E_G^{\{1,0\}} = 0.495t + 1.53\frac{t^2}{U}, \quad (26a)$$

$$E_G = -0.002t + 3.78\frac{t^2}{U}, \quad (26b)$$

TABLE V. UHF and CI (see text) energies of the Hubbard model in the 6×6 cluster for two holes (with respect to half-filling) and several values of U . All energies are given in units of the hopping integral t . The UHF results correspond to the configurations with the two holes at the shortest distance with either $S_z=0$ or 1 separated by lattice vector $(1,0)$ or $(1,1)$, respectively, and at the largest distance with $S_z=0$ holes separated by a $(2,3)$ vector. The CI results were obtained by including all configurations derived either from the set $\{1,0\}$ or $\{2,3\}$ (a total of 72 configurations), the set $\{1,1\}$ (36 configurations) all sets having $S_z=0$, namely, $\{1,0\}$, $\{2,1\}$, $\{3,0\}$, and $\{2,3\}$ (324 configurations), or all sets having $S_z=1$, i.e., $\{1,1\}$, $\{2,2\}$, $\{3,1\}$, and $\{3,3\}$ (117 configurations).

U/t	UHF			CI				
	$(1,0)$	$(2,3)$	$(1,1)$	$\{1,0\}$	$\{2,3\}$	$\{1,1\}$	All $S_z=0$	All $S_z=1$
6	-23.147	-23.121	-23.063	-23.704	-23.608	-23.352	-23.813	-23.700
8	-18.867	-18.920	-18.848	-19.488	-19.385	-19.075	-19.586	-19.448
20	-9.952	-10.260	-10.159	-10.525	-10.452	-10.285	-10.562	-10.479
200	-4.120	-4.632	-4.500	-4.622	-4.647	-4.510	-4.652	-4.650

where Eq. (26a) corresponds to holes at the shortest distance and Eq. (26b) to holes at the largest distance. Note that whereas in the case of the holes at the largest distance the gain goes to zero in the large- U limit, as for the isolated polaron, when the holes are separated by a $\{1,0\}$ vector, the gain goes to a finite value. This result is not surprising, as the following arguments suggest. The hopping terms in the bipolaron calculation, which are proportional to t at large U , describe the rotation of a pair around the position of one of the two holes. Each hole is spread between four sites. In order for a rotation to take place, one hole has to jump from one of these sites into one of the rotated positions. This process can always take place without a hole moving into a fully polarized site with the wrong spin. There is a gain in energy, even when $U/t \rightarrow \infty$. In the single-polaron case, the motion of a hole involves the inversion of, at least, one spin, which is fully polarized in the large- U limit. Because of this, hybridization gives a vanishing contribution to the energy as $U/t \rightarrow \infty$.

The results discussed above are in line with those for the width of the quasiparticle band. The numerical results can be fitted by

$$E_{\text{BW}}^{\{1,0\}} = 3.965t + 14.47\frac{t^2}{U}, \quad (27a)$$

$$E_{\text{BW}} = -0.007t + 10.1\frac{t^2}{U}, \quad (27b)$$

notation as in Eq. (26). Thus, the total bandwidth of the two bands obtained for holes in neighboring sites does not vanish in the infinite- U limit (as the energy gain reported in Fig. 2). The internal consistency of our calculations is shown comparing the large- U behavior of the two holes at the largest distance possible with the corresponding results obtained for the isolated polaron [compare this fitting with that given in Eq. (24)].

The hole-hole interaction, i.e., the difference between the energy of a state built up by all configurations with the two holes at the shortest distance (separated by a vector of the set $\{1,0\}$) and the energy of the state having the holes at the largest distance possible at a given cluster, is depicted in Fig. 4. Two holes bind for intermediate values of U .⁴⁴ This hap-

pens because the delocalization energy tends to be higher than the repulsive contribution obtained within mean field. The local character of the interactions is illustrated by the almost null dependence of the results shown in Fig. 4 on the cluster size.

The only numerical calculation which addresses the binding of holes in the Hubbard model is that of Ref. 8. The binding energy is defined as $\Delta = E_2 + E_0 - 2E_1$, where E_n is the ground state energy of the system with n holes. The results of Ref. 8 for the 4×4 cluster show that binding is favorable in the whole range of U explored; in particular Δ steadily decreases from $-0.00563t$ to $-0.0947t$ when U is varied from t to $50t$. Those authors also point out that for $U = \infty$, repulsion is found with $\Delta \approx 1.32t$. Our results for Δ , as defined in the preceding paragraph and for the same cluster, vary from $-0.039t$ to $-0.029t$ for $U = 4t - 50t$, with a maximum value of $-0.128t$ for $U = 8t$ (see Table II). The agreement with the results of Ref. 8 can be considered as satisfactory, once the differences in the definition of the binding energy and in the characteristics of the two calculations are taken into account. On the other hand, the absence of binding at infinite U reported in Ref. 8 is compatible with the results shown in Fig. 4. Similar calculations for the t - J model give binding between holes for $J/t \geq 0.1$.¹⁰ Taking $J = 4t^2/U$, this threshold agrees well with our results.

In order to clarify some aspects of the method, we have carried out a more detailed analysis of two-hole solutions in 6×6 clusters. The results are presented in Table V. Within the UHF approximation the most favorable solution is that with the two holes at the largest distance (2,3) but for the smallest U shown in Table V. The solution with the holes at the shortest distance (1,0) is only favored at small U , while for $U \geq 8$ even the solution with $S_z = 1$ has a smaller energy. Instead when the lattice symmetry is restored the solution with the holes at the shortest distance is the best for all U excluding $U = 200$. For such a large U the wave function constructed with all configurations from {2,3} has the lowest energy. The solution with $S_z = 1$ is unfavorable for all U shown in Table V, in contrast with the results found in the 4×4 cluster, indicating that size effects were determinant in the results for the smaller cluster. Including all configurations with S_z either 1 or 0 does not change this trend. The

TABLE VI. Absolute value of the interactions t_i and overlaps s_i between the configurations included in the case of two holes at the shortest distance, for several values of the interaction parameter U . The meaning of the symbols is given in Fig. 5. The results correspond to the 6×6 cluster.

U/t	t_1	t_2	t_3	s_1	s_2	s_3
8	2.459	4.672	1.202	0.124	0.235	0.056
20	1.418	1.624	0.159	0.119	0.135	0.009
200	0.646	0.651	0.007	0.088	0.088	9×10^{-5}
2000	0.584	0.584	7×10^{-4}	0.084	0.084	9×10^{-7}

small difference between the results for {1,0} and those with all configurations with $S_z = 0$ for large U is misleading. In fact, the weight of the configuration with the holes at the largest distance (2,3) in the final CI wave function increases with U . This will be apparent in the hole-hole correlations discussed in the following paragraph.

We have analyzed the symmetry of the ground state wave function $|\Psi\rangle$ obtained with all configurations having the holes at the shortest distance. The numerical results for all U show that $\langle \Phi^1 | \Psi \rangle = -\langle \Phi^2 | \Psi \rangle = \langle \Phi^3 | \Psi \rangle = -\langle \Phi^4 | \Psi \rangle$, where the $|\Phi^i\rangle$ are the four configurations shown in Fig. 2. This symmetry corresponds to the $d_{x^2-y^2}$ symmetry, in agreement with previous theoretical studies of the Hubbard and t - J models.^{11,45}

The quasiparticle band structure for two holes has also been investigated. The main interactions t_i and the overlaps s_i between the configurations are given in Table VI (the meaning of the symbols is specified in Fig. 2). The results correspond to a 6×6 cluster with the two holes at the shortest distance. At finite U many interactions contribute to the band; in Table VI we only show the largest ones. Of particular significance is the t_3 interaction which accounts for the simultaneous hopping of the two holes. This term, which clearly favors pairing, vanishes in the infinite- U limit, in line with the results for the hole-hole interaction (see above) which indicate that pairing is not favored at large U . Also in this limit $t_1 = t_2$. Including only the interactions given in Table VI, the bands can be easily obtained from

$$\begin{vmatrix} E + 2(s_1 E - t_1) \cos k_x + 2(s_3 E - t_3) \cos k_y & (s_2 E - t_2)(1 + e^{ik_x})(1 + e^{-ik_y}) \\ (s_2 E - t_2)(1 + e^{-ik_x})(1 + e^{ik_y}) & E + 2(s_1 E - t_1) \cos k_y + 2(s_3 E - t_3) \cos k_x \end{vmatrix} = 0. \quad (28)$$

Neglecting the overlap, the bands are given by

$$E(\mathbf{k}) = (t_1 + t_3)(\cos k_x + \cos k_y) \pm \sqrt{[(t_1 + t_3)(\cos k_x + \cos k_y)]^2 + 4t_2^2(1 + \cos k_x)(1 + \cos k_y)}. \quad (29)$$

In the infinite- U limit ($t_3 = 0$ and $|t_1| = |t_2|$) the bands are simply

$$E_1(\mathbf{k}) = -2t_1, \quad (30a)$$

$$E_2(\mathbf{k}) = 2t_1(1 + \cos k_x + \cos k_y). \quad (30b)$$

Note that, as in the single-hole case and due to the antiferromagnetic background, the bands have twice the lattice periodicity. The dispersionless band has also been reported in Ref. 35 and, in our case, it is a consequence of the absence of two-hole hopping in the infinite- U limit ($t_3 = 0$). Our results, however, disagree with the conclusions reached in Ref. 35 concerning the absence of hole attraction. We find a finite

TABLE VII. Hole-hole correlations $\langle(1-n_i)(1-n_j)\rangle$ as a function of the hole-hole distance r_{ij} for three values of U . The results correspond to two holes in 6×6 clusters and were obtained including all configurations of the set $\{1,0\}$. The normalization $\sum_j \langle(1-n_i)(1-n_j)\rangle=1$ was used.

r_{ij}/U	$8t$	$20t$	$200t$
0	1.4	0.657	0.491
1	-0.171	-2.51×10^{-3}	3.27×10^{-2}
$\sqrt{2}$	3.99×10^{-2}	6.30×10^{-2}	6.97×10^{-2}
2	2.0×10^{-3}	1.43×10^{-3}	3.97×10^{-4}
$\sqrt{5}$	9.6×10^{-3}	9.55×10^{-3}	9.54×10^{-3}
$2\sqrt{2}$	3.34×10^{-3}	8.43×10^{-4}	7.53×10^{-4}
3	4.54×10^{-3}	4.18×10^{-3}	6.03×10^{-3}
$\sqrt{10}$	2.46×10^{-3}	6.66×10^{-4}	7.53×10^{-4}
$\sqrt{13}$	1.49×10^{-3}	8.51×10^{-4}	7.53×10^{-4}

attraction for holes at intermediate U 's. It is interesting to note that our effective hopping is of order t , and not of order t^2/U as in Ref. 35. This effect is due to the delocalized nature of the single-polaron texture (five sites, at least), and it does not correspond to a formally similar term which can be derived from the mapping from the Hubbard to the t - J model.⁴⁶

The results for the hole-hole correlation, $\langle(1-n_i)(1-n_j)\rangle$, as function of the hole-hole distance $r_{ij}=|\mathbf{r}_i-\mathbf{r}_j|$ are reported in Tables VII and VIII. The normalization $\sum_j \langle(1-n_i)(1-n_j)\rangle=1$ has been used. The results correspond to CI wave functions with $S_z=0$ and were obtained including all configurations from either the set $\{1,0\}$ or from the sets $\{1,0\}$, $\{1,2\}$, $\{3,0\}$, and $\{2,3\}$. The results are in qualitative agreement with those in Ref. 8. When comparing with results obtained for the t - J model, one must take into account that, in the Hubbard model, the hole-hole correlation, as defined above, can take negative values (see the Appendix). This is due to the appearance of configurations with doubly occupied sites, which are counted as negative holes. Aside from this effect, our results describe well a somewhat puzzling result found in the t - J model (see, for instance, Refs. 13, 30, and 47) and in small clusters of the Hubbard model:⁸ the maximum hole-hole correlation occurs when the two holes are in the same sublattice, at a distance equal to $\sqrt{2}$ times the lattice spacing.⁴⁸ This result follows directly from the delo-

TABLE VIII. As in Table VII, but including all configurations from the sets $\{1,0\}$, $\{2,1\}$, $\{3,0\}$, and $\{2,3\}$.

r_{ij}/U	$8t$	$20t$	$200t$
0	1.367	0.664	0.493
1	-0.183	-1.08×10^{-2}	5.18×10^{-3}
$\sqrt{2}$	2.38×10^{-2}	5.18×10^{-2}	7.65×10^{-3}
2	4.37×10^{-3}	3.06×10^{-3}	2.36×10^{-2}
$\sqrt{5}$	8.57×10^{-3}	8.99×10^{-3}	1.59×10^{-2}
$2\sqrt{2}$	9.48×10^{-3}	5.20×10^{-3}	7.48×10^{-3}
3	1.30×10^{-2}	7.47×10^{-3}	4.43×10^{-2}
$\sqrt{10}$	8.86×10^{-3}	4.64×10^{-3}	2.36×10^{-2}
$\sqrt{13}$	1.74×10^{-2}	6.4×10^{-3}	5.06×10^{-3}

TABLE IX. UHF and CI energies (in units of the hopping integral t) for four holes in 10×10 clusters and several values of the interaction U . The results correspond to configurations with either the four holes on a square (denominated as 4) or on two bipolarons (2+2) separated by a (5,5) vector.

U/t	4		2+2	
	UHF	CI	UHF	CI
8	-50.500	-50.828	-50.782	-51.242
16	-29.208	-29.629	-29.922	-30.321
32	-17.588	-17.989	-18.574	-18.921
128	-8.651	-9.005	-9.851	-10.148
512	-6.406	-6.744	-7.659	-7.941
4096	-5.750	-6.084	-7.020	-7.297

calized nature of the spin polarons, as seen in Fig. 1. The center of each spin polaron propagates through one sublattice only, but the electron cloud has a finite weight in the other one, even when $U/t\rightarrow\infty$. This effect is noted in all cases but for $U=200t$ with all configurations. In that case there is not a clear maximum and the correlations are appreciable even at rather large distances. The reason for this behavior is that for large U the configuration with the holes at the largest distance, namely, $\{2,3\}$, has the lowest energy and, thus, a large weight in the CI wave function. This is consistent with the fact that no attraction was observed at large U (see Fig. 4). The slower decrease with distance of hole-hole correlations, obtained for $U=8t$ including configurations from the four sets (Table VIII), may be a consequence of the decrease in the difference between UHF and CI energies as U diminishes (see Fig. 4). Finally, note that the correlation function shows a better defined peak at a distance of $\sqrt{2}$ the lattice constant, for $U=20t$ (see Tables VII and VIII, particularly the latter). This is in agreement with remarks of Ref. 8 in the sense that the most favorable range for binding was $U=16t-20t$.

C. Four holes

An interesting question is whether the holes would tend to segregate when more holes are added to the cluster. In order to investigate this point, we have calculated total energies for four holes on 10×10 clusters with the holes either centered on a square or located on two bipolarons separated by a (5,5) vector and with the holes at the shortest distance. Two (four) configurations (plus translations) were included in each case. In the case of two bipolarons only configurations in which the two bipolarons are rotated simultaneously are included. Other possible configurations have different energies and contribute to a lesser extent to the wave function. In any case, increasing the size of the basis set would not have changed the essential conclusion of our analysis (see below). The results for several values of U are shown in Table IX. We note that already at the UHF level the solution with two separated bipolarons has a lower energy. The Coulomb repulsion term in the Hamiltonian does not favor the configuration with the aggregated holes but for very small U . Restoring lattice symmetry decreases the energy in both cases to an amount which in neither case vanishes in the infinite- U limit. The decrease is slightly larger in the case of the four

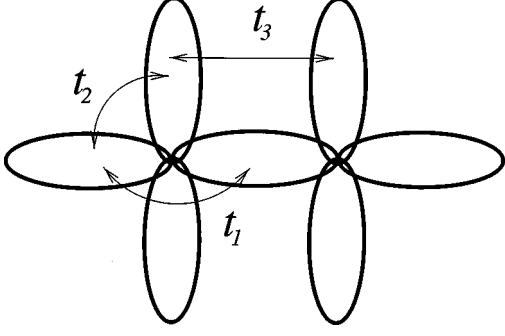


FIG. 5. Interactions between two-hole configurations having the holes at the shortest distance [separated by a (1,0) vector].

holes on a square. This result can be understood by noting that the holes move more freely (producing the smallest distortion to the AF background) when the charge is confined to the smallest region possible. In any case, this is not enough to compensate the rather important difference in energy between the two cases at the UHF level. These results indicate that for large and intermediate U no hole segregation takes place and that the most likely configuration is that of separated bipolarons.

D. Effective Hamiltonian for hole pairing

As discussed above, in the large- U limit the bipolaron moves over the whole cluster due to the interactions among the four mean field wave functions of Fig. 2 (interactions t_1 and t_2 in Fig. 5). This mechanism can be viewed as another manifestation of hole-assisted hopping. The possibility of hole-assisted hopping has been already considered in Ref. 49, although in a different context. It always leads to superconductivity. In our case, we find a contribution, in the large- U limit, of the type

$$\mathcal{H}_{hop} = \sum \Delta t c_{i,j;\sigma}^\dagger c_{i,j;\sigma} (c_{i+1,j;\bar{\sigma}}^\dagger c_{i,j+1;\bar{\sigma}} + c_{i-1,j;\bar{\sigma}}^\dagger c_{i+1,j;\bar{\sigma}}) + \text{H.c.} + \text{perm}. \quad (31)$$

This term admits the BCS decoupling

$$\Delta t \langle c_{i,j;\sigma}^\dagger c_{i+1,j;\bar{\sigma}}^\dagger \rangle c_{i,j;\sigma} c_{i,j+1;\bar{\sigma}} + \text{H.c.} + \dots$$

It favors superconductivity with either s - or d -wave symmetry, depending on the sign of Δt . Since we find $\Delta t > 0$, d -wave symmetry follows.

VI. CONCLUDING REMARKS

We have analyzed the leading corrections to the Hartree-Fock solution of the Hubbard model, with zero, one, and two holes. We show that a mean field approach gives a reasonable picture of the undoped system for the entire range of values of U/t .

The main drawback of mean field solutions in doped systems is their lack of translational invariance. We overcome this problem by using the configuration-interaction method. In the case of one hole, the localized spin polaron is replaced by delocalized wave functions with a well-defined dispersion

relation. The bandwidth, in the large- U limit, scales as t^2/U , and the solutions correspond to spin polarons delocalized in a given sublattice only. As in the undoped case, these results are in good agreement with other numerical calculations, for the Hubbard and t - J models.

The same approach is used to analyze the interactions between pairs of holes. We first obtain Hartree-Fock solutions with two holes at different separations. From comparing their respective energies, and also with single-hole solutions, we find a short-range repulsive interaction between holes. This picture is significantly changed when building delocalized solutions. The energy gain from the delocalization is enough to compensate the static, mean field, repulsion. There is a net attractive interaction for $8 \leq U/t \leq 50$, approximately. The correlations between the holes which form this bound state are in good agreement with exact calculations, when available. The state has $d_{x^2-y^2}$ symmetry. In this range of parameters, we find no evidence of hole clustering into larger structures.

Further proof of the efficiency of the present CI approach results from a comparison with the CI approach of Ref. 29, which is based upon an extended basis (\mathbf{k} space). For a 6×6 cluster and $U=4t$ the UHF localized solution has an energy of -31.747 . A CI calculation including 36 localized configurations lowers the energy down to -31.972 . This has to be compared with the result reported in Ref. 29 obtained by means of 2 027 860 extended configurations, namely, -30.471 . The difference between the two approaches should further increase for larger U .

We have not applied the same technique to other Hartree-Fock solutions which have been found extensively in the Hubbard model: domain walls separating antiferromagnetic regions.^{21,50-52} The breakdown of translational symmetry associated with these solutions is probably real and not just an artifact of the Hartree-Fock solution, as in the previous cases. Hybridization of equivalent solutions can, however, stabilize domain walls with a finite filling, which are not the mean field solutions with the lowest energy.

Because of the qualitative differences between spin polarons and domain walls, we expect a sharp transition between the two at low values of U/t . Note, however, that the scheme presented here, based on mean field solutions plus corrections, is equally valid in both cases.

ACKNOWLEDGMENTS

Financial support from the CICYT, Spain, through Grant Nos. PB96-0875, PB96-0085, and PB95-0069, is gratefully acknowledged.

APPENDIX: HOLE-HOLE CORRELATIONS IN THE HYDROGEN MOLECULE

Here we explicitly calculate the hole-hole correlations in the hydrogen molecule described by means of the Hubbard model. Let us call a_σ^\dagger and b_σ^\dagger the operators that create a particle with spin σ at sites a and b , respectively. The ground state wave function has $S_z=0$ and is given by

$$|\psi\rangle = (2 + \alpha^2)^{-1/2} (|\phi_1\rangle + |\phi_2\rangle + |\phi_3\rangle), \quad (A1)$$

where,

$$|\phi_1\rangle = a_{\uparrow}^{\dagger} b_{\downarrow}^{\dagger} |0\rangle, \quad (\text{A2a})$$

$$|\phi_2\rangle = \frac{1}{\sqrt{2}}(a_{\uparrow}^{\dagger} a_{\downarrow}^{\dagger} + b_{\uparrow}^{\dagger} b_{\downarrow}^{\dagger}) |0\rangle, \quad (\text{A2b})$$

$$|\phi_3\rangle = b_{\uparrow}^{\dagger} a_{\downarrow}^{\dagger} |0\rangle, \quad (\text{A2c})$$

with

$$\alpha = \frac{E}{\sqrt{2}}, \quad E = \frac{U}{2} - \left(\frac{U^2}{4} + 4 \right)^{1/2}. \quad (\text{A3})$$

The wave functions in Eqs. (A2) are orthonormalized, namely, $\langle \phi_i | \phi_j \rangle = \delta_{ij}$. The result for the hole-hole correlations on different sites is

$$\langle \psi | (1 - n_a)(1 - n_b) | \psi \rangle = -\frac{\alpha^2}{2 + \alpha^2}. \quad (\text{A4})$$

As $\alpha = -\sqrt{2}, 0$ when $U = 0, \infty$, this expectation value varies from -0.5 to 0.0 . Thus it can take negative values as found in the case of clusters of the square lattice. Instead, the hole-hole correlation on the same site is given by

$$\langle \psi | (1 - n_a)(1 - n_a) | \psi \rangle = \frac{\alpha^2}{2 + \alpha^2}, \quad (\text{A5})$$

which is positive for all values of U . Particle-particle correlations are obtained by adding 1 to these results.

-
- ¹A. P. Kampf, Phys. Rep. **249**, 219 (1994).
²D. J. Scalapino, Phys. Rep. **250**, 329 (1995).
³N. Bulut, D. J. Scalapino, and S. R. White, Phys. Rev. Lett. **72**, 705 (1994).
⁴R. Preuss, W. Hanke, and W. van der Linden, Phys. Rev. Lett. **75**, 1344 (1995).
⁵E. Dagotto, A. Nazarenko, and M. Boninsegni, Phys. Rev. Lett. **73**, 728 (1994).
⁶P. W. Leung and R. J. Gooding, Phys. Rev. B **52**, R15 711 (1995).
⁷D. Duffy, A. Nazarenko, S. Haas, A. Moreo, J. Riera, and E. Dagotto, Phys. Rev. B **56**, 5597 (1997).
⁸G. Fano, F. Ortolani, and A. Parola, Phys. Rev. B **42**, 6877 (1990).
⁹M. Boninsegni and E. Manousakis, Phys. Rev. B **47**, 11 897 (1993).
¹⁰D. Poilblanc, J. Riera, and E. Dagotto, Phys. Rev. B **49**, 12 318 (1994).
¹¹E. Dagotto, Rev. Mod. Phys. **66**, 763 (1994).
¹²K. Kuroki and H. Aoki, cond-mat/9710019 (unpublished).
¹³C. Gazza, G. B. Martins, J. Riera, and E. Dagotto, Phys. Rev. B **59**, R709 (1999).
¹⁴A. V. Dotsenko, Phys. Rev. B **57**, 6917 (1998).
¹⁵S. Zhang, J. Carlson, and J. E. Gubernatis, Phys. Rev. Lett. **78**, 4486 (1997).
¹⁶E. Louis, G. Chiappe, J. Galán, F. Guinea, and J. A. Vergés, Phys. Rev. B **48**, 426 (1993).
¹⁷E. Louis, G. Chiappe, F. Guinea, J. A. Vergés, and E. V. Anda, Phys. Rev. B **48**, 9581 (1993).
¹⁸E. Louis, F. Guinea, M. P. López-Sancho, and J. A. Vergés, Europhys. Lett. **44**, 229 (1998).
¹⁹G. Seibold, E. Sigmund, and V. Hizhnyakov, Phys. Rev. B **57**, 6937 (1998).
²⁰G. Seibold, Phys. Rev. B **58**, 15 520 (1998).
²¹J. A. Vergés, E. Louis, P. S. Lomdahl, F. Guinea, and A. R. Bishop, Phys. Rev. B **43**, 6099 (1991).
²²F. Guinea, E. Louis, and J. A. Vergés, Phys. Rev. B **45**, 4752 (1992).
²³J. E. Hirsch, Phys. Rev. Lett. **59**, 228 (1987).
²⁴A. Kampf and J. R. Schrieffer, Phys. Rev. B **41**, 6399 (1990).
²⁵E. Dagotto and J. R. Schrieffer, Phys. Rev. B **43**, 8705 (1991).
²⁶A. Auerbach, *Interacting Electrons and Quantum Magnetism* (Springer-Verlag, New York, 1994).
²⁷E. Louis, J. Galán, F. Guinea, J. A. Vergés, and J. Ferrer, Phys. Status Solidi B **173**, 715 (1992).
²⁸A. Ramsak and P. Horsch, Phys. Rev. B **57**, 4308 (1998).
²⁹B. Friedman and G. Levine, Phys. Rev. B **55**, 9558 (1997).
³⁰S. R. White and D. J. Scalapino, Phys. Rev. B **55**, 6504 (1997).
³¹R. B. Laughlin, cond-mat/9709195 (unpublished).
³²P. W. Anderson and G. Baskaran, cond-mat/9711197 (unpublished).
³³R. Chitra and G. Kotliar, cond-mat/9811144 (unpublished).
³⁴E. Dagotto and T. M. Rice, Science **271**, 618 (1996).
³⁵E. W. Carlson, S. A. Kivelson, Z. Nussinov, and V. J. Emery, Phys. Rev. B **57**, 14 704 (1998).
³⁶A. W. Sandvik, Phys. Rev. B **56**, 11 678 (1997).
³⁷In the following we use parentheses to denote a single lattice vector (m, n) and curly brackets to refer to the full set of vectors $\{m, n\}$.
³⁸G. Martínez and P. Horsch, Phys. Rev. B **44**, 317 (1991).
³⁹Z. Liu and E. Manousakis, Phys. Rev. B **51**, 3156 (1995).
⁴⁰B. M. Elrick and A. E. Jacobs, Phys. Rev. B **52**, 10 369 (1995).
⁴¹M. Vojta and K. W. Becker, Phys. Rev. B **57**, 3099 (1998).
⁴²J. Altmann, W. Brenig, A. P. Kampf, and E. Müller-Hartmann, Phys. Rev. B **52**, 7395 (1995).
⁴³G. Polatssek and K. W. Becker, Phys. Rev. B **55**, 1408 (1997).
⁴⁴Note that at large U the ferromagnetic solution sets in. In Ref. 16 it was shown that the energy of two holes in a ferromagnetic $L \times L$ cluster could be fitted by $E/t = -7.942 + 31.02/L^2$. Comparing the present numerical results with this energy gives a transition to the ferromagnetic solution approximately at $U/t = 32$, for the cluster sizes investigated here.
⁴⁵M. Cyrot and D. Pavuna, *Introduction to Superconductivity and High- T_c Materials* (World Scientific, Singapore, 1992).
⁴⁶S. A. Trugman, Phys. Rev. B **37**, 1597 (1988).
⁴⁷J. Riera and E. Dagotto, Phys. Rev. B **57**, 8609 (1997).
⁴⁸Note that this result is obtained without including configurations which clearly favor it, such as that proposed in Ref. 47 in which the two holes lie on neighboring sites along a diagonal and a neighboring spin is flipped.
⁴⁹J. E. Hirsch, Phys. Rev. B **48**, 3327 (1993).
⁵⁰J. Zaanen and O. Gunnarsson, Phys. Rev. B **40**, 7391 (1989).
⁵¹D. Poilblanc and T. M. Rice, Phys. Rev. B **39**, 9749 (1989).
⁵²H. J. Schulz, Phys. Rev. Lett. **64**, 1445 (1990).